Automatic identification of Diabetic Macular Edema biomarkers using Optical Coherence Tomography scans

Joaquim de Moura[1,2*], Gabriela Samagaio[1,2], Jorge Novo[1,2], Pablo Charlón[3], María Isabel Fernández[4,5,6], Francisco Gómez-Ulla[4,5,6], and Marcos Ortega[1,2]
{joaquim.demoura, gabriela.samagaio, jnovo, mortega}@udc.es
pcharlon@sgoc.es
{maribelfernandez, franciscogomez-ulla}@institutogomez-ulla.es

[1] Department of Computer Science, University of A Coruña, A Coruña, (Spain)
[2] CITIC - Research Center of Information and Communication Technologies, University of A Coruña, A Coruña, (Spain)
[3] Instituto Oftalmológico Victoria de Rojas, A Coruña, (Spain)
[4] Instituto Oftalmológico Gómez-Ulla, Santiago de Compostela, (Spain)
[5] Department of Ophthalmology, Complejo Hospitalario Universitario de Santiago, Santiago de Compostela, (Spain)
[6] University of Santiago de Compostela, Santiago de Compostela, (Spain)

Abstract. Optical Coherence Tomography (OCT) imaging has revolutionized the daily clinical practice, especially in the field of ophthalmology. Diabetic Macular Edema (DME) is one of the most important complications of diabetes and a leading cause of preventable blindness in the developed countries. In this way, a precise identification and analysis of DME biomarkers allow the clinical specialists to make a more accurate diagnosis and treatment of this relevant ocular disease.
Thus, in this work, we present a computational system for the automatic identification and extraction of DME biomarkers by the analysis of OCT scans, following the clinical classification of reference in the ophthalmological field. The presented method was validated using a dataset composed by 40 OCT images that were retrieved from different patients. Satisfactory results were obtained, providing a consistent and coherent set of different computational biomarkers that can help the clinical specialists in their diagnostic procedures.

Keywords: Computer-aided diagnosis, Optical Coherence Tomography, Diabetic Macular Edema, biomarkers

1 Introduction

Diabetic Macular Edema (DME) represents a leading cause of visual impairment and blindness among the working-age individuals in the developed countries [1]. DME is one of the most common eye diseases that is associated with diabetes

mellitus, affecting the 12% of type 1 and the 28% of type 2 diabetic patients [2]. This relevant disease is characterized by an abnormal retinal thickness produced by intraretinal fluid accumulations, also called Macular Edemas (MEs), within the retinal tissues. In this context, the use of Computer-Aided Diagnosis (CAD) systems is crucial, as it provides useful information for the clinical specialists to assess the severity of the DME pathology. In particular, in ophthalmology, Optical Coherence Tomography (OCT) has become an important clinical tool that is commonly used for the analysis and interpretation of many retinal structures and ocular disorders [3–5].

OCT is a well-established medical imaging technique that is capable of providing high-resolution cross-sectional tomographic images of biological tissues by measuring the intensity of the back-scattered light [6]. In this way, these images are widely used by the clinical specialists in the diagnosis and monitoring of the DME disease, permitting a complete analysis of the retinal morphology and their histopathology properties in real time and non-invasively.

Using the OCT image modality as reference, Otani *et al.* [7] proposed a clinical classification of the MEs associated with DME into 3 pathological types: Serous Retinal Detachment (SRD), Cystoid Macular Edema (CME) and Diffuse Retinal Thickening (DRT). This clinical classification is based on the different fluid accumulation patterns derived from the DME disease and that can be differentiated in the OCT images. Figure 1 presents an illustrative example of an OCT image with the simultaneous presence of the 3 defined types of the DME disease.

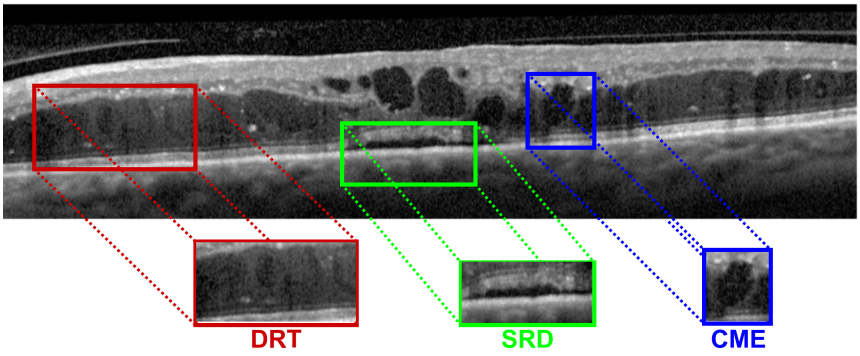

Fig. 1. Example of an OCT image with the simultaneous presence of the 3 defined types of DME: DRT, SRD and CME.

Posteriorly, Panozzo *et al.* [8] complemented the Otani classification using the presence of the Epiretinal Membrane (ERM) to better characterize the DME disease in the OCT images. Hence, ERM is a relevant disorder of the vitreoretinal interface that is also associated with DME disease. In particular, the ERM presence is defined by a response of the immune system to protect the retina from changes of the vitreous humour. Consequently, this response provokes that the

cells of the retina converge on the inner retinal surface, producing a translucent membrane, which can thicken or contract. Figure 2 shows an illustrative example of an OCT image with the presence of the ERM membrane.

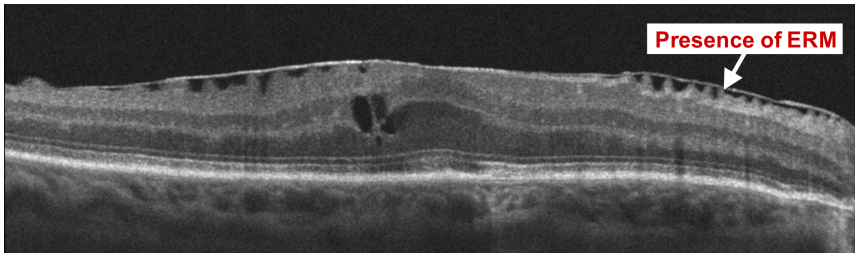

Fig. 2. Example of an OCT image with the presence of the ERM membrane.

In this context, an automatic system for the identification and analysis of different computational biomarkers of the DME disease facilitates the work of the clinical specialists, reducing the costs of medical care and improving the quality of life of patients.

Given the relevance of this ocular pathology, some computational proposals were presented focusing their studies in the automatic identification of the presence of DME cases using the OCT scans as source of information. As reference, Sidibé *et al.* [9] employed a Gaussian Mixture Models (GMM) for the identification of patients with DME using OCT images. In particular, the method models the appearance of normal OCT images with a GMM model and detects pathological OCT images as outliers. Quellec *et al.* [10] proposed a methodology using a set of texture features that were extracted to characterize different retinal tissues. Then, a learning strategy was applied using a k-NN classifier for the identification of CME edemas in the macular region. Wilkins *et al.* [11] developed a method for the identification of the ERM presence through manual labeling in the OCT images performed by the clinical specialist, which allowed the computer tool to measure the retinal thickness around the labeled region. As we can observe, the presented methods only aimed at the partial identification of DME cases without addressing the problem of the extraction of relevant computational biomarkers for their clinical utility in predictive, preventive and personalized medicine.

Thus, in this work, we present a fully automatic system for the identification and extraction of DME biomarkers using OCT scans, following the clinical classification of reference in the ophthalmological field [7, 8]. To achieve this, firstly, the system segments the main retinal layers to delimit 3 retinal regions in the OCT scan. Then, the system identify the presence of ME (SRD, CME and DRT) and ERM cases within the corresponding retinal region. To do so, the system combines and exploits different clinical knowledge (position, dimension, shape and morphology) with image processing and machine learning strategies. Finally, using these localizations as source of information, the system derives

different computational biomarkers that can help the clinical specialists in their diagnostic procedures.

This paper is organized as follows: Section 2 includes the detailed characteristics of the proposed methodology. Next, the results are presented, explained and discussed in Section 3. Finally, Section 4 depicts the general conclusions and the possible future lines of work.

2 Methodology

As illustrated in Fig. 3, the designed methodology is divided into 4 main stages. Firstly, the system segments the main retinal layers. Posteriorly, the system delimits 3 retinal regions: ILM/OPL, OPL/ISOS and ISOS/RPE regions. Regarding the MEs, the system localizes and extracts the relevant biomarkers of each ME type within these retinal regions. Regarding the ERM, a complementary strategy was implemented for the identification and subsequent extraction of the corresponding computational biomarkers.

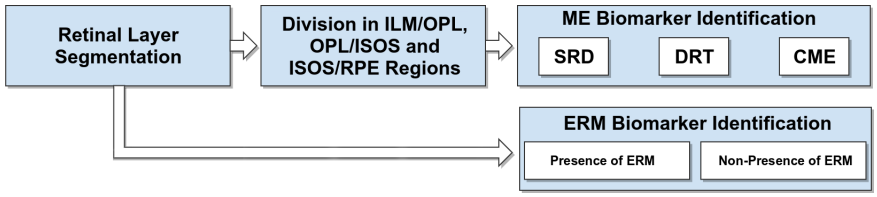

Fig. 3. Main structure of the proposed methodology.

2.1 Retinal Layer Segmentation

In this work, 4 main retinal layers were identified, since they provide the correct delimitation of the retinal regions where the different types of ME and ERM usually appear. These retinal layers are: the Inner Limiting Membrane (ILM), the Retinal Pigment Epithelium (RPE), the junction of the Inner and Outer Segments (ISOS) and the Outer Plexiform Layer (OPL). In particular, to extract the ILM, RPE and ISOS layers, we follow the work proposed by González-López *et al.* [12]. To do that, the method employs an active contour-based model to segment these retinal boundaries. For the OPL layer, we designed a different strategy based on a region growing approach to obtain the corresponding region with similar intensity properties [13]. As result of this strategy, the upper limits of the extracted region represents the OPL layer. Figure 4 shows a representative example of OCT image with the segmentation of the aimed retinal layers.

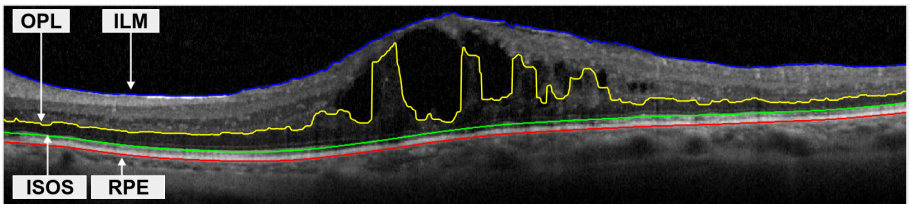

Fig. 4. Example of an OCT image with the segmentation of the aimed 4 retinal layers: ILM, OPL, ISOS and RPE.

2.2 Division in ILM/OPL, OPL/ISOS and ISOS/RPE Regions

Using the previous retinal layer identifications, 3 representative regions of interest are identified and extracted: ILM/OPL, OPL/ISOS and ISOS/RPE regions, as illustrated in Fig. 5. Generally, the SRD edemas appear as a dome-shape area in the ISOS/RPE region. DRT edemas usually appear in the OPL/ISOS region whereas CME edemas are frequently present in the ILM/OPL region. In more severe stages of the DME disease, CME edemas can also proliferate in the OPL/ISOS region.

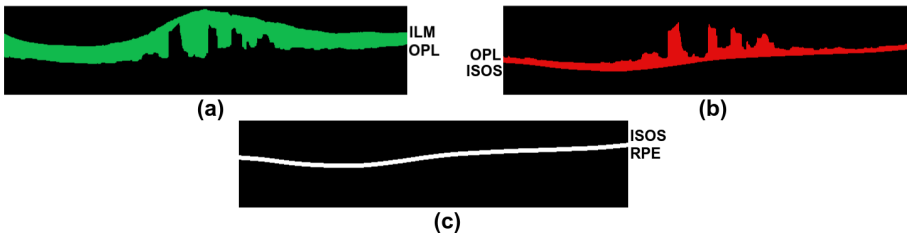

Fig. 5. Illustrative example of the division of the regions of interest. (a) Delimitation of the ILM/OPL region. (b) Delimitation of the OPL/ISOS region. (c) Delimitation of the ISOS/RPE region.

2.3 ME Biomarker Identification

The proposed methodology includes different strategies to perform a simultaneous identification of each type of ME (SRD, CME and DRT) within the corresponding retinal region. To do that, we follow the work proposed by Samagaio *et al.* [13], given their adequate results for this issue. For the SRD and CME cases, we apply an adaptive multilevel thresholding algorithm, whereas for the DRT case a machine learning strategy was implemented. Then, a list composed of different clinical knowledge (position, dimension, shape and morphology) is used to reduce the set of possible false identifications. As output, the method provides a labeled OCT image with the precise identification of each ME type for a better characterization of the present DME disease. Finally, the method extracts

and analyzes different ME biomarkers according to their relative position within the OCT scans. These ME biomarkers are: number of SRDs, number of CMEs, number of DRT columns, relative position of SRDs, relative position of CMEs and relative position of DRTs. As we can see in Fig. 6, these ME biomarkers are extracted in the foveal region (1.0 mm diameter central circle area), parafoveal region (ring area between 1.0 and 3.0 mm in diameter) and perifoveal region (ring area between 3.0 and 6.0 mm in diameter). These regions were established according to clinical criteria [14].

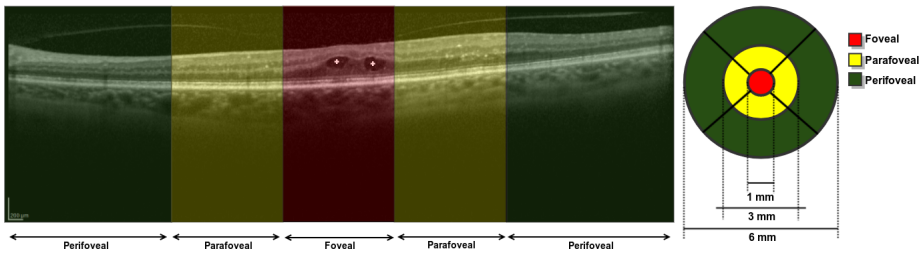

Fig. 6. Example of an OCT image with the extraction of ME biomarkers where 2 CME regions were identified in the foveal region.

2.4 ERM Biomarker Identification

Using the previously segmented ILM layer, we perform the precise identification of the presence or non-presence of ERM cases using the OCT scans. To achieve this, we based our proposal in the work of Baamonde *et al.* [15]. Firstly, the system extracts a set of relevant features from the search space, including intensity, texture and domain-related clinical features. Then, a machine learning strategy is used to train and test the potential of discrimination of the presented method. Using these identifications, the system derives different ERM biomarkers considering its relative position within the OCT scans, as seen on Fig 7. In particular, these ERM biomarkers imply: absolute and relative number of ERM columns and relative position of ERMs.

3 Experimental Results

The proposed system was validated using a dataset consisting of 40 OCT images retrieved from different patients, being 20 acquired with a Spectralis OCT confocal scanning laser ophthalmoscope from Heidelberg Engineering and 20 obtained with a CIRRUS OCT from Carl Zeiss Meditec. Each OCT image was labeled by an expert clinician, identifying regions with the presence of ME as well as ERM. To measure the efficiency of the proposed method, we evaluated the identification of the different DME biomarkers according to their relative localization within the OCT scans, as show in Table 1. As we can see, the method

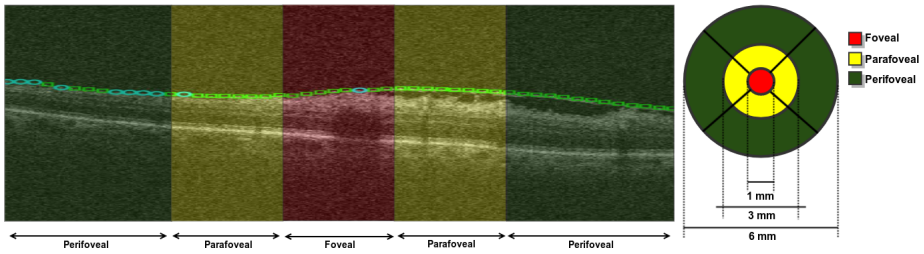

Fig. 7. Example of an OCT image with the extraction of ERM biomarkers where the presence of ERM was identified in all regions of the retina.

achieved satisfactory results, returning in a coherent way the values of the DME identifications for the foveal, parafoveal and parafoveal retinal regions.

Table 1. Performance of the method for the identification of DME biomarkers.

	(%) SRDs	(%) CMEs	(%) DRT columns	(%) ERM columns
Foveal	100%	34.28%	22.43%	9.92%
Parafoveal	0%	54.28%	47.77%	28.01%
Perifoveal	0%	11.42%	29.79%	62.05%

4 Discussion and Conclusions

OCT has proven to be a robust medical imaging modality that provides cross-sectional tomographic scans that are commonly used for clinical specialists in the analysis and evaluation of DME. This relevant ocular disease is one of the most common causes of blindness in individuals with diabetes. In this context, we presented a fully automatic system for the identification and extraction of DME biomarkers using OCT scans, following the clinical classification of reference in the ophthalmological field. To do that, the presented method exploits different image processing and machine learning strategies to identify the presence of ME (SRD, CME and DRT) and cases of ERM from patients with DME disease. Subsequently, the system derives different computational biomarkers that may lead to the early diagnosis and treatment of this relevant ocular disease. The validation was performed using 40 OCT images from two representative ophthalmological devices. The presented system achieved satisfactory results, demonstrating its suitability to be used in real clinical scenarios.

Acknowledgments This work is supported by the Instituto de Salud Carlos III, Government of Spain and FEDER funds through the DTS18/00136 research project and by the Ministerio de Economía y Competitividad, Government of Spain through the DPI2015-69948-R research project. Also, this work has received financial support

from the European Union (European Regional Development Fund - ERDF) and the Xunta de Galicia, Centro singular de investigación de Galicia accreditation 2016-2019, Ref. ED431G/01; and Grupos de Referencia Competitiva, Ref. ED431C 2016-047.

References

1. R. Lee, T. Y. Wong, and C. Sabanayagam. Epidemiology of diabetic retinopathy, diabetic macular edema and related vision loss. *Eye and vision*, 2(1):17, 2015.
2. P. Romero-Aroca. Managing diabetic macular edema: the leading cause of diabetes blindness. *World Journal of Diabetes*, 2(6):98, 2011.
3. J. de Moura, J. Novo, P. Charlón, N. Barreira, and M. Ortega. Enhanced visualization of the retinal vasculature using depth information in OCT. *Medical & Biological Engineering & Computing*, 55(12):2209–2225, 2017.
4. J. de Moura, J. Novo, J. Rouco, M. G. Penedo, and M. Ortega. Automatic identification of intraretinal cystoid regions in Optical Coherence Tomography. In *Conf. on Artificial Intelligence in Medicine in Europe*, pages 305–315. Springer, 2017.
5. J. de Moura, J. Novo, S. Penas, M. Ortega, J. Silva, and A. M. Mendonça. Automatic Characterization of the Serous Retinal Detachment Associated with the Subretinal Fluid Presence in Optical Coherence Tomography Images. *Procedia Computer Science*, 126:244–253, 2018.
6. J. Schmitt. Optical Coherence Tomography (OCT): a review. *IEEE Journal of selected topics in quantum electronics*, 5(4):1205–1215, 1999.
7. T. Otani, S. Kishi, and Y. Maruyama. Patterns of Diabetic Macular Edema with Optical Coherence Tomography. *Amer. J. of Ophthalmology*, 127(6):688–693, 1999.
8. G. Panozzo, B. Parolini, E. Gusson, A. Mercanti, S. Pinackatt, G. Bertoldo, and S. Pignatto. Diabetic macular edema: an OCT-based classification. In *Seminars in Ophthalmology*, volume 19, pages 13–20. Taylor & Francis, 2004.
9. D. Sidibe, S. Sankar, G. Lemaitre, M. Rastgoo, J. Massich, C. Cheung, G. Tan, D. Milea, E. Lamoureux, T. Y Wong, et al. An anomaly detection approach for the identification of DME patients using spectral domain optical coherence tomography images. *Computer Methods and Programs in Biomedicine*, 139:109–117, 2017.
10. G. Quellec, K. Lee, M. Dolejsi, M. Garvin, M. Abramoff, and M. Sonka. Three-dimensional analysis of retinal layer texture: identification of fluid-filled regions in SD-OCT of the macula. *IEEE Trans. on Medical Imaging*, 29(6):1321–1330, 2010.
11. J. Wilkins, C. Puliafito, M. Hee, J. Duker, E. Reichel, J. Coker, J. Schuman, E. Swanson, and J. Fujimoto. Characterization of epiretinal membranes using Optical Coherence Tomography. *Ophthalmology*, 103(12):2142–2151, 1996.
12. A. González-López, J. de Moura, J. Novo, M. Ortega, and M. G. Penedo. Robust segmentation of retinal layers in Optical Coherence Tomography images based on a multistage active contour model. *Heliyon*, 5(2):e01271, 2019.
13. G. Samagaio, A. Estévez, J. de Moura, J. Novo, I. Fernández, and M. Ortega. Automatic Macular Edema identification and characterization using OCT images. *Computer Methods and Programs in Biomedicine*, 163:47–63, 2018.
14. S. Othman, F. Manan, A. Zulkarnain, Z. Mohamad, and A. Ariffin. Macular thickness as determined by optical coherence tomography in relation to degree of myopia, axial length and vitreous chamber depth in malay subjects. *Clinical and Experimental Optometry*, 95(5):484–491, 2012.
15. S. Baamonde, J. de Moura, J. Novo, and M. Ortega. Automatic detection of epiretinal membrane in OCT images by means of local luminosity patterns. In *Int. Work-Conference on Art. Neural Networks*, pages 222–235. Springer, 2017.